Stereoselective Organometallic Reactions: A Force Field Study of π-Allyl Intermediates in Nickel(0)-Catalyzed Cycloadditions[1]

M. M. Gugelchuk*[,2] **and K. N. Houk***

Contribution from the Department of Chemistry, University of Waterloo, Waterloo, Ontario N2L 3G1, Canada, and Department of Chemistry and Biochemistry, University of California, Los Angeles, California 90024

Received January 19, 1993. Revised Manuscript Received October 8, 1993[●]

Abstract: A fully flexible, quantitative model based on Allinger's MM2 force field has been developed to predict diastereoinduction in intramolecular nickel-catalyzed [4 + 4] cycloadditions. The position of all atoms are optimized with a force field consisting of MM2 parameters for normal atoms and new parameters for atoms attached to the metal. The new parameters for MM2 were derived from crystallographic data augmented by *ab initio* calculations where experimental data were lacking. Application of this new force field to a number of test complexes demonstrates that the method can be used to predict molecular structures for these systems and that the π-allyl parameters are transferable to other square-planar metal complexes. Initial modeling studies on the conformational preferences of species relevant to nickel-catalyzed cyclodimerizations are presented. Molecular mechanics calculations on various proposed organonickel species suggest that stereoselectivity can be reproduced by consideration of the energies of stereoisomeric anti-η^1,η^3-bis-allylic nickel phosphine complexes. Predictions of new stereoselectivities are made for several systems.

Introduction

In recent years, extensive applications of molecular mechanics methods such as MM2[3] to predict molecular geometries and energetics for a wide variety of organic and biochemical problems have been reported. This technique can be applied to any system by careful parametrization. Our particular interests have involved the development of force fields for the modeling of transition states of stereoselective organic reactions.[4] Because of the explosive growth of synthetic methods involving asymmetric transformations mediated by transition metals,[5] we became interested in applying molecular mechanics methods to investigate the factors influencing the stereoselectivities of organometallic reactions.

Relatively little has been published on successful applications of empirical force field methods to transition metal compounds[6] and even less on applications to π-bonded organometallic complexes.[7] This is largely due to widely recognized complications in the conventional methods of (1) defining unique bond angles and their corresponding equilibrium values, (2) strong electronic effects on the idealized molecular geometries, and (3) in the case of π-coordinated organic ligands, defining the point of attachment to the metal. As a result, new force field programs attempting to resolve these problems are making their appearance (e.g., UFF,[6a] SHAPES,[6b] MMX,[6i] YETI,[6h] etc.). Recently, Bosnich *et al.* reported a force field for the structures and vibrational spectroscopy of linear metallocenes.[7e] The program most frequently used to study the structure and stabilities of conformations and diastereomers in typical organic compounds is Allinger's MM2 program[3] and variations of it. In spite of certain inadequacies in potential functions and parameters which are being addressed in newer force fields such as MM3,[8] we have augmented parameters to MM2 to make it immediately applicable to calculations on a wide variety of square-planar π-allyl metal complexes.

Our initial efforts have been directed toward modeling the diastereoselective nickel(0)-catalyzed [4 + 4] cycloaddition reactions reported by Wender.[9] Intramolecular nickel-catalyzed diene dimerizations have furnished a highly stereoselective route for the direct construction of cyclooctanoid bicyclic systems. Initial results demonstrated that the length of the chain connecting the tetraene had a profound influence on the stereochemistry of the resulting ring fusion. A three-atom tether leads to cis-fused bicyclo[6.3.0]undecadiene products, while a four-atom tether gives nearly exclusive formation of trans-fused bicyclo[6.4.0]dodecadienes. The effect of stereogenic centers along the

* Abstract published in *Advance ACS Abstracts*, December 1, 1993.

(1) Presented in part at the 199th National ACS Meeting, Boston, MA, April 22–28, 1990, Abstract ORGN-411.

(2) Address correspondence to this author at the University of Waterloo.

(3) (a) Allinger, N. L.; Yuh, Y. *QCPE* **1980**, *12*, 395. (b) Burkert, U.; Allinger, N. L. *Molecular Mechanics*; ACS Monograph Series 177; American Chemical Society: Washington, DC, 1982.

(4) See, for example: (a) Wu, Y.-D.; Wang, Y.; Houk, K. N. *J. Org. Chem.* **1992**, *57*, 1362–1369. (b) González, J.; Taylor, E. C.; Houk, K. N. *J. Org. Chem.* **1992**, *57*, 3753–3755. (c) Wu, Y.-D.; Houk, K. N.; Florez, J.; Trost, B. M. *J. Org. Chem.* **1991**, *56*, 3656–3664. (d) Broeker, J. L.; Houk, K. N. *J. Org. Chem.* **1991**, *56*, 3651–3655. (e) Zipse, H.; He, J.; Houk, K. N.; Giese, B. *J. Am. Chem. Soc.* **1991**, *113*, 5006–5017. (f) Wu, Y.-D.; Houk, K. N.; Valentine, J. S.; Nam, W. *Inorg. Chem.* **1992**, *31*, 718–720.

(5) (a) Liebeskind, L. S. *Advances in Metal-Organic Chemistry*; JAI Press: Greenwich, CT, 1991. (b) Harrington, P. J. *Transition Metals in Total Synthesis*; Wiley: New York, 1990, and references therein.

(6) See: (a) Rappé, A. K.; Casewit, C. J.; Colwell, K. S.; Goddard, W. A., III; Skiff, W. M. *J. Am. Chem. Soc.* **1992**, *114*, 10024–10035. (b) Allured, V. S.; Kelly, C. M.; Landis, C. R. *J. Am. Chem. Soc.* **1991**, *113*, 1–12. (c) Pozigun, D. V.; Kuz'min, V. E. *Zh. Strukt. Khim.* **1988**, *29*, 171–172. (d) Vedani, A.; Dobler, M.; Dunitz, J. D. *J. Comput. Chem.* **1986**, *7*, 701–710. (e) Brecknell, D. J.; Raber, D. J.; Ferguson, D. M. *THEOCHEM* **1985**, *124*, 343–351. (f) Brubaker, G. R.; Johnson, D. W. *Coord. Chem. Rev.* **1984**, *53*, 1–53 and references therein. (g) Gajewski, J. J.; Gilbert, K. E.; McKelvey, J. In *Advances in Molecular Modeling*; Liotta, D., Ed.; JAI Press: Greenwich, CT, 1990; Vol. 2, pp 65–92. (h) Vedani, A. *J. Comput. Chem.* **1988**, *9*, 269–280.

(7) (a) Davies, S. G.; Derome, A. E.; McNally, J. P. *J. Am. Chem. Soc.* **1991**, *113*, 2854–2861. (b) Bogdan, P. L.; Irwin, J. J.; Bosnich, B. *Organometallics* **1989**, *8*, 1450–1453. (c) Brown, J. M.; Evans, P. L. *Tetrahedron* **1988**, *44*, 4905–4916. (d) Timofeeva, T. V.; Solovokhotov, Yu. L.; Struchkov, Yu. T. *Dokl. Akad. Nauk SSSR* **1987**, *294*, 1173–1176. (e) Doman, T. N.; Landis, C. R.; Bosnich, B. *J. Am. Chem. Soc.* **1992**, *114*, 7264–7272.

(8) (a) Allinger, N. L.; Yuh, Y. H.; Lii, J.-H. *J. Am. Chem. Soc.* **1989**, *111*, 8551–8566. (b) Lii, J.-H.; Allinger, N. L. *J. Am. Chem. Soc.* **1989**, *111*, 8566–8575. (c) Lii, J.-H.; Allinger, N. L. *J. Am. Chem. Soc.* **1989**, *111*, 8576–8582.

(9) (a) Wender, P. A.; Ihle, N. C. *J. Am. Chem. Soc.* **1986**, *108*, 4678–4679. (b) Wender, P. A.; Snapper, M. L. *Tetrahedron Lett.* **1987**, *28*, 2221–2224. (c) Wender, P. A.; Ihle, N. C. *Tetrahedron Lett.* **1987**, *28*, 2451–2454. (d) Wender, P. A.; Ihle, N. C.; Correia, C. R. D. *J. Am. Chem. Soc.* **1988**, *110*, 5904–5906. (e) Wender, P. A.; Tebbe, M. J. *Synthesis* **1991**, 1089–1094.

π-*Allyl Intermediates in Ni(0)-Catalyzed Cycloadditions*

J. Am. Chem. Soc., Vol. 116, No. 1, 1994 331

Scheme 1. Diastereoselective Intramolecular Nickel-Catalyzed [4 + 4] Cycloadditions
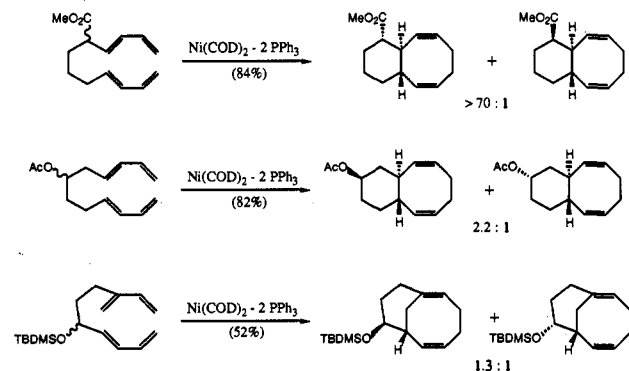
connecting tether is particularly interesting. Allylic substituents gave high diastereoinduction, especially the carbomethoxy group.[9a] In contrast, homoallylic substitution provided very little diastereoselectivity (Scheme 1). Further investigations suggested the extent of diastereoinduction was dependent on the steric nature of the allylic substituents rather than their coordinative nature.[9c]

Assuming we would be able to rationalize the diastereoinduction in nickel-catalyzed cycloadditions in terms of steric interactions among the various reactive conformations of ground-state or transition-state nickel complexes, we set out to develop force field models which could reliably reproduce the known structures of π-allyl nickel phosphine species. This paper reports the development of a force field for this type of complex which we believe provides reliable MM2 parameters for these π-bonded transition metal species.[10] The results of our initial application of force field methods toward the study of stereoselectivity in nickel-catalyzed intramolecular [4 + 4] cycloadditions are also presented.

Background

The nickel-catalyzed [4 + 4] cycloaddition reaction is believed to occur in a stepwise manner through a complex sequence involving a number of nickel-bonded intermediates. An idealized mechanism, developed from years of extensive study[11] involving product analysis and stoichiometric reactions, is outlined for the butadiene cyclodimerization in Figure 1. The mechanistic picture can be broadly summarized as two 1,3-diene molecules undergo oxidative coupling at a nickel(0) center to form bis-allyl nickel intermediates (**1** and **2**) which react further by reductive elimination, possibly through the corresponding bis-η[1]-allyl forms (**3**), to give the cyclic products. Over the years, some doubt has been cast on the plausibility of the initial diene coupling directly forming the bis-η[3]-allyl complex (**2**). Experimental and theoretical data have suggested the actual coupling product may be better formulated as the η[1],η[3]-bis-allyl complex (**1**).[12,13] Yet despite nearly thirty years of continuing investigations, there is still a great lack of specific details concerning what in fact occurs during this transformation.
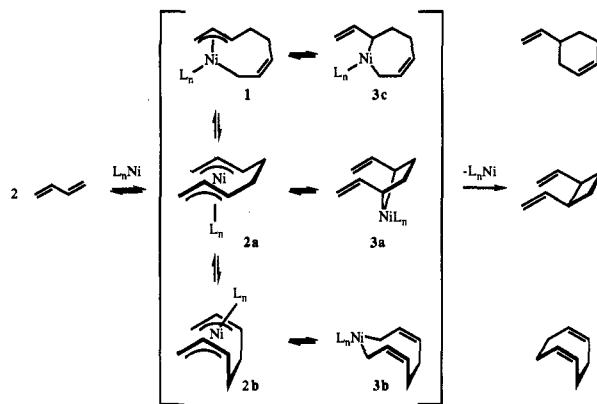

Figure 1. Idealized mechanism of nickel-catalyzed cyclodimerization of butadiene.

The hapticity and configuration[14] of the bis-allyl chain are thought to control the course of the reaction: vinylcyclohexene would arise from the syn-η[3]-allyl-cis-η[1]-allyl form, **1**, divinylcyclobutane from the syn-bis-η[3]-allyl form, **2a**, and cyclooctadiene from the anti-bis-η[3]-allyl form, **2b**. While it is clear how the configuration of the bis-allyl form is reflected in the corresponding product types, the question as to the actual hapticity in the product-determining intermediate is still open for debate. These types of complexes are known to exist in a dynamic equilibrium between the σ- and π-forms, and one would expect rapid isomerization of the σ- and π-allyl forms to occur under the reaction conditions (cf. Figure 1).[15,16]

Hapticity preferences have been strongly linked to the electronic character[17] of the phosphorus ligand. Basic phosphines are known to stabilize the η[1],η[3]-bis-allyl form, while the less basic phosphites stabilize the bis-η[3]-allyl forms.[11,18] There is also a significant steric effect in operation. The use of a phosphorus ligand having high steric requirements[17] increases the formation of cyclooctadiene. From an energetic standpoint, the bis-syn isomer (e.g., **2a**)[14] is typically the more thermodynamically stable of the two types of bis-η[3]-allyl complexes, but steric interactions can drive the equilibrium in favor of the bis-anti form. Substituents on the allyl ligand will further modify both the electron density at the metal and the steric requirements of these species. However any analysis is subject to the usual caveat that the catalytically active species may not be the most stable form of these complexes but may be a less stable, more reactive form.

(14) Stereochemical nomenclature for bis-η[3]-allyl systems:
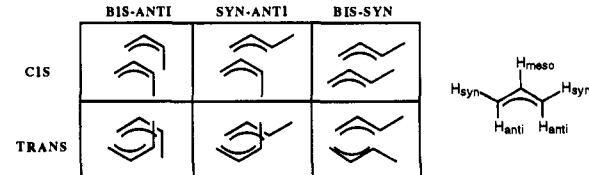
(15) (a) Jolly, P. W. In *Comprehensive Organometallic Chemistry*; Wilkinson, G., Stone, F. G. A., Abel, E. W., Eds.; Pergamon: New York, 1982; Vol. 6, pp 81–85, 145–182. (b) Henc, B.; Jolly, P. W.; Salz, R.; Wilke, G.; Benn, R.; Hoffmann, E. G.; Mynott, R.; Schroth, G.; Seevogel, K.; Sekutowski, J. C.; Krüger, C. *J. Organomet. Chem.* **1980**, *191*, 425–448. (c) Henc, B.; Jolly, P. W.; Salz, R.; Stobbe, S.; Wilke, G.; Benn, R.; Mynott, R.; Seevogel, K.; Goddard, R.; Krüger, C.; *J. Organomet. Chem.* **1980**, *191*, 449–475. (d) Lehmkuhl, H.; Rufinska, A.; Mehler, K.; Benn, R.; Schroth, G. *Liebigs Ann. Chem.* **1980**, 744–753. (e) Lehmkuhl, H.; Rufinska, A.; Benn, R.; Schroth, G.; Mynott, R. *Liebigs Ann. Chem.* **1981**, 317–332. (f) Tolman, C. A. *J. Am. Chem. Soc.* **1970**, *92*, 6777–6784. (g) Tolman, C. A. *J. Am. Chem. Soc.* **1970**, *92*, 6785–6790.

(16) See: Deeming, A. J. In *Mechanisms of Inorganic and Organometallic Reactions*; Twigg, M. V., Ed.; Plenum: New York, 1983; Vol. 1, pp 249–271 and references therein.

(17) Tolman, C. A. *Chem. Rev.* **1977**, *77*, 313–348.

(18) (a) Vrieze, K.; van Leeuwen, P. W. N. M. *Prog. Inorg. Chem.* **1971**, *14*, 1–63. (b) van Leeuwen, P. W. N. M.; Praat, A. P. *J. Organomet. Chem.* **1970**, *21*, 501–515.

(10) While this manuscript was under review, a similar parametrization effort was reported. See: Norrby, P.-O.; Akermark, B.; Haeffner, F.; Hansson, S.; Blomberg, M. *J. Am. Chem. Soc.* **1993**, *115*, 4859–4867.

(11) (a) Jolly, P. W.; Wilke, G. *The Organic Chemistry of Nickel*; Academic: New York, 1975; Vol. II, pp 133–161. (b) Jolly, P. W. In *Comprehensive Organometallic Chemistry*; Wilkinson, G., Stone, F. G. A., Abel, E. W., Eds.; Pergamon: New York, 1970; Vol. 8, pp 671–679. (c) Wilke, G. *Angew. Chem., Int. Ed. Engl.* **1988**, *27*, 185–206.

(12) (a) Heimbach, P.; Jolly, P. W.; Wilke, G. *Adv. Organomet. Chem.* **1970**, *8*, 29–86. (b) Heimbach, P. *Aspects Homogeneous Catal.* **1975**, *2*, 79–158.

(13) (a) van Leeuwen, P. W. N. M.; Roobeek, C. F. *Tetrahedron* **1981**, *37*, 1973–1983. (b) Graham, C. R.; Stephenson, L. M. *J. Am. Chem. Soc.* **1977**, *99*, 7098–7100. (c) Buchholz, H.; Heimbach, P.; Hey, H.; Selbeck, H.; Wiese, W. *Coord. Chem. Rev.* **1972**, *8*, 129–138. (d) Braterman, P. S. *Top. Curr. Chem.* **1980**, *92*, 149–172.

A particularly intriguing mechanistic point and the focus of this investigation is the nature of the nickel species involved in the stereochemically discriminating step of the catalytic process. This issue, which has not been addressed by the proposed mechanism, is crucial to perfecting and extending synthetic applications of the intramolecular reaction. Some attempts have been made to interpret stereochemistry by the use of frontier orbitals under the assumption that each step in the reaction sequence is concerted and invoking the Woodward–Hoffmann rules.[12,13] The general mechanistic picture outlined for butadiene is expected to be valid for the intramolecular variant. Wender's observations of the same effects of nickel to phosphine ratio and ligand structure on the type of product formed lend support to this assumption.[9a,d] The intramolecular nature of this system would impose some limits to the possible orientations of the organic ligand about the metal. The hapticity in the product-determining species may also be influenced by the geometric and conformational limitations of these substrates.

Due to the complexity of this reaction mechanism and the current scarcity of detailed information concerning the actual nickel-bonded intermediates, we undertook a theoretical investigation to provide some clues for a greater understanding of this transformation. The choice of intermediates to test was based on several factors. First, the actual number of coordinated ligands, L_n, is uncertain. For the cyclodimerization reaction to be successful, at least one of the coordination sites around the zerovalent nickel must be occupied by a donor ligand (preferably a phosphine or phosphite ligand).[11,12] All isolable organonickel complexes from stoichiometric reactions contain a single phosphine ligand. It is likely, however, that the association and dissociation of a second [phosphine] ligand may play a key role in promoting the bond reorganizations.

Secondly, neglecting the assortment of different hapticity combinations, there are two types of organonickel intermediates proposed in the general mechanism: bis-diene and bis-allyl. Little is known about the structure of the initial Ni(diene)$_2$L$_n$ complexes, and numerous bonding possibilities exist. The structures of the bis-η^1-allyl nickel complexes are unknown. While they are commonly proposed as intermediates (cf. Figure 1), they have never been detected in any of these reactions. The bis-η^3-allyl and the η^1,η^3-bis-allyl types of complexes have been isolated and are well characterized.[11] This allowed us to use empirical data to parameterize a force field to reproduce these structures.

The observed diastereoselection in Wender's systems could result from either thermodynamically or kinetically controlled formation or collapse of one of the nickel intermediates. If thermodynamic control is dominant, the product stereochemistries will depend only on the free energy differences in the ground states of diastereomeric complexes. However, if kinetic control dominates, the product stereochemistries will depend on the differences in activation energies of competing transition states. If ground-state preferences are maintained in the isomeric transition structures, our ground-state models may provide greater insight into the factors influencing the stereochemistry of this reaction and guide us to the appropriate transition-state model. The questions of thermodynamic versus kinetic control at each of the individual steps have yet to be completely unraveled, and there also remains the possibility that the mechanism may be different for different substrates.

In an attempt to better understand the origins of the stereoselectivity, Wender and Ihle conducted MM2 calculations on the diastereomeric products.[9c] The more thermodynamically stable diastereomers (according to MM2) were the major products of the reaction, but there was no correlation between the steric energy differences and the observed product ratios. When a simple, strictly organic model was used to approximate the steric environments of proposed bis-η^3-allyl nickel intermediates, better

G	Calc Ratio (G$_{eq}$: G$_{ax}$)	Obsd Ratio (G$_{eq}$: G$_{ax}$)
CN	1.2 : 1	1.5 : 1
CH$_3$	28 : 1	20 : 1
CH$_2$OAc	29 : 1	21 : 1
CO$_2$Me	38 : 1[a]	>70 : 1

(a) P. Wender, personal communication.

Figure 2. Comparison of Wender model with observed product ratios.

agreement of the calculated energy differences with experimental product distributions was obtained (Figure 2). However, this model still failed to provide a satisfactory explanation for the greatly enhanced selectivity exhibited by the carbomethoxy group.

Having no *a priori* reason to draw conclusions about the hapticity in the product-determining species, we chose to investigate the geometrical and conformational characteristics of the syn- and anti-η^1,η^3-bis-allyl and bis-η^3-allyl nickel species. We have compared these to the experimental results on the stereochemistries of the reaction to ascertain their role in controlling stereoselectivity in the nickel-catalyzed [4 + 4] cycloadditions. As the following results will show, steric interactions in only one type of these nickel intermediates successfully reproduce quantitatively the observed diastereoselectivities. The experimental data are rather limited. As more experimental data with substituted tetraenes is gathered, more stringent tests and further refinement of this model will be possible.

Results and Discussion

I. Development of Allyl Nickel Model Systems. Flexible MM2 models were constructed with the π-allyl ligand modeled as occupying two coordination sites being symmetrically bound to nickel through the terminal carbon atoms. The positions of all atoms were optimized with a force field of MM2 parameters for normal atoms[19] and new parameters for those attached to the metal. Stretching and bending parameters for π-allyl nickel complexes were developed on the basis of existing crystallographic data. To quantify the rotational barriers of syn and anti substituents on the π-allyl nickel fragment, as well as about nickel–phosphorus and σ-bonded carbon–nickel bonds, we performed *ab initio* calculations on various nickel species using the Gaussian 88/90 suite of programs and basis sets contained therein.[20] Full details of this parametrization effort will be published elsewhere. The quality of our new parameters was gauged by comparisons of crystallographic and computed structures. Starting structures for the optimizations were taken from crystallographic coordinates. In order to make sure this did not bias the results, additional optimizations were performed with input structures drawn freehand using the graphical interface provided in PCMODEL.[21]

A total of five unique crystal structures[22] (Figure 3) was used to test how well the new parameter set reproduced the crystal-

(19) The MM285 parameter set was used for all normal atoms. For the five-coordinate bis-π-allyl complexes, a dummy atom held fixed at the coordinates of the metal atom was used to specifically exclude evaluation of deformation angles between the two allyl moieties. Only one allyl group was attached to the dummy atom via the terminal carbons, and the dummy atom parameters were equated to those developed for the metal, except for the van der Waals radius, which was set to 0.0001.

(20) (a) Frisch, M. J.; Head-Gordon, M.; Trucks, G. W.; Foresman, J. B.; Schlegel, H. B.; Raghavachari, K.; Robb, M. A.; Binkley, J. S.; Gonzalez, C.; Defrees, D. J.; Fox, D. J.; Whiteside, R. A.; Seeger, R.; Melius, C. F.; Baker, J.; Martin, R. L.; Kahn, L. R.; Stewart, J. J. P.; Topiol, S.; Pople, J. A. *Gaussian 90*, Revision F; Gaussian, Inc.: Pittsburgh, PA, 1990. (b) Frisch, M. J.; Head-Gordon, M.; Schlegel, H. B.; Raghavachari, K.; Binkley, J. S.; Gonzalez, C.; Defrees, D. J.; Fox, D. J.; Whiteside, R. A.; Seeger, R.; Melius, C. F.; Baker, J.; Martin, R. L.; Kahn, L. R.; Stewart, J. J. P.; Fluder, E. M.; Topiol, S.; Pople, J. A. *Gaussian 88*, Revision C; Gaussian, Inc.: Pittsburgh, PA, 1988.

(21) *PCMODEL*, Version 4; Serena Software: Bloomington, IN, 1990.

(22) (a) Barnett, B.; Büssemeier, B.; Heimbach, P.; Jolly, P. W.; Krüger, C.; Tkatchenko, I.; Wilke, G. *Tetrahedron Lett.* **1972**, *15*, 1457–1460. (b) Cameron, T. S.; Prout, C. K. *Acta Crystallogr.* **1972**, *B28*, 2021–2028. (c) Brandes, H.; Goddard, R.; Jolly, P. W.; Krüger, C.; Mynott, R.; Wilke, G. *Z. Naturforsch.* **1984**, *39b*, 1139–1150. (d) Barnett, B. L.; Krüger, C. *J. Organomet. Chem.* **1974**, *77*, 407–421.
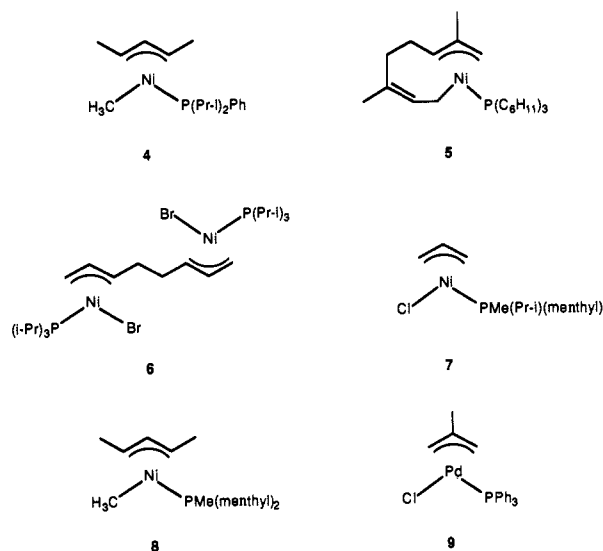
π-Allyl Intermediates in Ni(0)-Catalyzed Cycloadditions

J. Am. Chem. Soc., Vol. 116, No. 1, 1994 333

Figure 3. Square-planar π-allyl complexes used to test the force field parameters.

lographic geometries. Common to all five structures (**4–8**) is a square-planar π-allyl nickel phosphine element. The fourth ligand completing the arrangement is methyl, σ-allyl, chloride, or bromide. Bond angle parameters involving this fourth ligand remained identical regardless of the actual identity of this ligand. To test the transferability of these parameters to other square-planar metal complexes, a suitable π-allyl palladium complex[23] (**9**) was also examined. The only alterations necessary for complex **9** were three metal–ligand bond distance parameters (e.g., Pd–Cl, Pd–P, and Pd–$C_{\pi,t}$), which were increased by 0.1 Å to account for the longer bond lengths of the second-row transition metal.

In general, the MM2-minimized geometries and crystallographic geometries were in impressive agreement (Table 1). The expected deviations were those due to strong electronic influences on the metal–ligand bond lengths, since our parameters were designed for a symmetrically bound π-allyl ligand. We made no attempt to incorporate the trans influence common in these types of transition metal complexes. To do so requires the equilibrium bond length and force constant parameters about nickel to be adjusted on a case by case basis depending on both the electronic nature of the respective trans ligands and their arrangement in the complex of interest. However, the largest deviations were those involving the L'–M–P and P–M–$C_{\pi,t}$ trans bond angles and are likely due to the idealized square-planar geometry built into the parameter set.

One concern to be addressed is the geometry with respect to the central π-allyl carbon, $C_{\pi,c}$. Since our model does not explicitly attach this carbon to the metal center, there are no bond distance or angle parameters with respect to the metal to influence its position in the optimized geometries. The expectation was that since all other geometric parameters of the π-allyl moiety were explicitly included in the model, this would constrain the central carbon close to the desired position, and indeed that was found to be the case. In general, the bond angles involving $C_{\pi,c}$ and the metal were very well predicted in the MM2 calculated geometries. The $C_{\pi,c}$–Ni distances are slightly overestimated as were the $C_{\pi,t}$–Ni distances. However, it is interesting to note that the relative bond lengths of the π-allyl fragment to the metal (e.g., the central carbon is closer than the terminal carbons) are reproduced by this force field even without the explicit Ni–$C_{\pi,c}$ bond. This result was gratifying, not only for a general reduction in the amount of new parameters needed but also in that it allows for transfer of these π-allyl parameters to metal geometries other than square planar with a minimum of bond angle adjustments.

(23) Faller, J. W.; Blankenship, C.; Whitmore, B.; Sena, S. *Inorg. Chem.* **1985**, *24*, 4483–4490.

Table 1. Experimental and MM2 Calculated Geometric Parameters

interaction	X-ray av	MM2 av	RMSD
Bond Lengths (Å)			
Ni–$C_{\pi,t}$	2.058	2.076	0.019
Ni–$C_{\pi,c}$	2.005	2.056	0.057
Ni–P	2.190	2.192	0.003
Ni–C_{sp^3}	1.980	1.987	0.009
$C_{\pi,c}$–$C_{\pi,t}$	1.411	1.421	0.006
$C_{\pi,t}$–C_{sp^3} syn	1.492	1.499	0.004
Ni–Br	2.311	2.331	0.028
Bond Angles (deg)			
$C_{\pi,c}$–$C_{\pi,t}$–C_{sp^3} syn	123.2	123.6	1.2
Ni–$C_{\pi,t}$–C_{sp^3} syn	128.1	127.6	1.6
H_a–$C_{\pi,t}$–C_{sp^3} syn	116.9	114.7	2.5
$C_{\pi,t}$–$C_{\pi,c}$–$C_{\pi,t}$	119.1	119.9	1.1
Ni–$C_{\pi,t}$–$C_{\pi,c}$	68.1	69.1	1.1
Ni–$C_{\pi,c}$–$C_{\pi,t}$	72.2	70.7	1.5
$C_{\pi,t}$–Ni–$C_{\pi,t}$	72.4	72.7	0.4
$C_{\pi,c}$–Ni–$C_{\pi,t}$	39.3	40.1	1.0
P–Ni–$C_{\pi,t}$ trans	167.1	172.4	6.0
P–Ni–$C_{\pi,t}$ cis	97.7	100.0	2.8
P–Ni–$C_{\pi,c}$	134.2	133.6	1.9
L'–Ni–$C_{\pi,t}$ trans	163.7	166.2	3.1
L'–Ni–$C_{\pi,t}$ cis	91.8	94.1	2.5
L'–Ni–$C_{\pi,c}$	126.1	128.3	3.1
L'–Ni–P	98.0	93.2	5.3
Ni–P–C_{sp^3}	114.2	114.0	2.9
H–C_σ–Ni	108.2	110.1	3.2
H_a–$C_{\pi,t}$–Ni	98.8	95.0	4.1
H_a–$C_{\pi,t}$–$C_{\pi,c}$	113.8	118.0	4.9
H–$C_{\pi,c}$–$C_{\pi,t}$	117.7	119.0	1.4
$C_{\pi,t}$–C_{sp^3} syn–C_{sp^3}	115.4	116.1	0.8
C_{sp^3}–$C_{\pi,c}$–$C_{\pi,t}$	120.9	119.6	2.2

Bis-η^3-allyl Nickel Phosphine Complexes. Our initial model calculations used PH₃ or PMe₃ to limit complications arising from conformational energy differences of the organic ligands. There is no reason other than complexity of calculations that the actual phosphine of Wender's studies (e.g., PPh₃) was not used. Indeed, our studies of simple complexes included the actual phosphine, and we also include the triphenylphosphine ligand to our working models for the intramolecular complexes at a later stage (*vide infra*).

Investigations of the conformational preferences of cisoid bis-η^3-allyl complexes were carried out using flexible models derived from modification of the crystal structure of bis-η^3-allyl-(trimethylphosphine)nickel.[15c] Only the deformation angles within each individual allyl–metal unit were explicitly evaluated. This allowed us to use our new π-allyl metal parameters with no additional parameters and only one change, that being the angle of the terminal allyl carbons with the phosphorus atom about the metal center. The $C_{\pi,t}$–Ni–P angle was set to 104.5° for square-pyramidal and 90.0°/120.0° for trigonal-bipyramidal nickel centers. The MM2-optimized structures of the square-pyramidal bis-syn (**10**) and bis-anti (**11**) complexes are shown in Figure 4.

There is some distortion of the square-pyramidal geometry about the metal. This is consistent with the geometries of known five-coordinate π-allyl nickel complexes.[15c,22c,24] The two η^3-allyl ligands are approximately parallel to each other. A slight twist of one allyl group away from parallel is seen, which allows the ethano bridge connecting the two allyl groups to adopt a somewhat staggered conformation, thereby reducing the C–H eclipsing interactions. The energy difference between these two structures was 4.6 kcal/mol favoring the bis-syn form.

A third structural type, anti-bis-η^3-allyl (**12**), in which the two allyl moieties are mutually trans, was also examined. The MM2-minimized structure is shown in Figure 4. Due to the anti

(24) (a) Barnett, B. L.; Krüger, C.; Tsay, Y.-H. *Angew. Chem., Int. Ed. Engl.* **1972**, *11*, 137–138. (b) Sirigu, A. *Inorg. Chem.* **1970**, *9*, 2245–2249. (c) Walther, D.; Dinjus, E.; Sieler, J.; Thanh, N. N.; Schade, W.; Leban, I. *Z. Naturforsch.* **1983**, *38B*, 835–840. (d) Churchill, M. R.; O'Brien, T. A. *J. Chem. Soc. A* **1970**, 206–212.
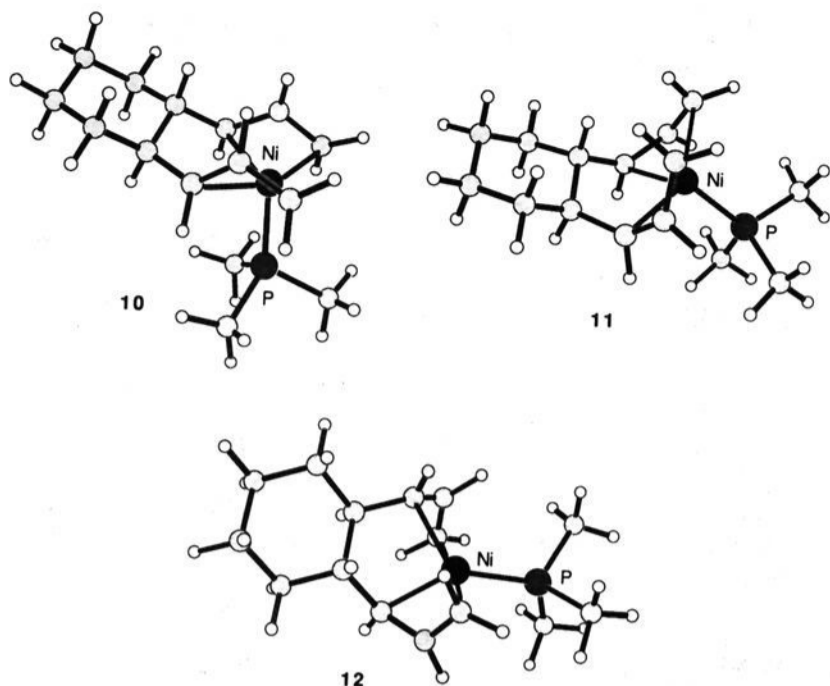
Figure 4. MM2-minimized structures of model complexes **10**, **11**, and **12**.
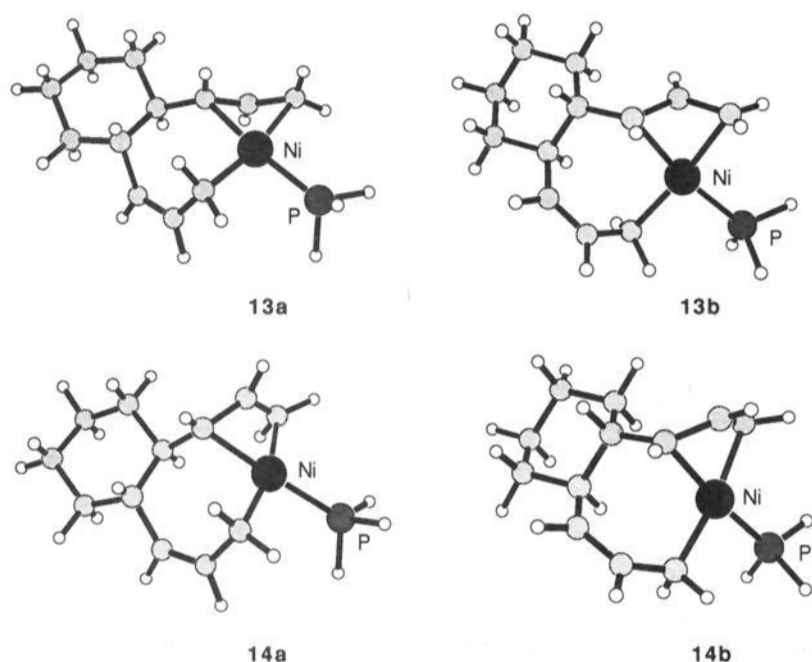

Figure 5. MM2-minimized structures of model complexes **13** and **14**.

configurations and the transoid orientation, a trigonal bipyramidal geometry about the metal was more geometrically accessible. In this model each π-allyl spans across axial–equatorial positions, with the unsubstituted allyl termini in the axial positions. The small bite angle of the bidentate allyl ligand ($\approx 72°$) necessarily distorts the trigonal-bipyramidal bond angles. The calculated geometry of the organic ligand is in good agreement with that of a similar transoid anti-bis-η^3-octadienyl ruthenium dicarbonyl complex.[25] This structure was found to be 1.0 kcal/mol more stable than the corresponding cisoid bis-anti complex **11**. For comparison, in the simpler complex, bis-π-allylnickel, the transoid isomer is about 0.7 kcal/mol lower in energy than the cisoid isomer.[11b]

The η^1,η^3-bis-allyl chain is more conformationally flexible than those in their bis-η^3-allyl counterparts. Two different orientations are possible for the η^1-allyl moiety: (1) the endo form in which the central carbon of the η^3-allyl and the double bond are on the same side of the plane containing the nickel and terminal allyl carbons or (2) the exo form in which the central carbon of the η^3-allyl and the double bond are on opposite sides of the plane containing the nickel and terminal allyl carbons. Optimized structures are shown in Figure 5. Results of our calculations predict the endo conformation (as in **13a** and **14b**) to be more stable by 1.6 kcal/mol for the syn-allyl system and the exo conformation (as in **13b** and **14a**) to be more stable by 2.1 kcal/

(25) Cox, D. N.; Roulet, R.; Chapius, G. *Organometallics* **1985**, *4*, 2001–2005.

Scheme 2. Relationship of Substituent to Product Concavity
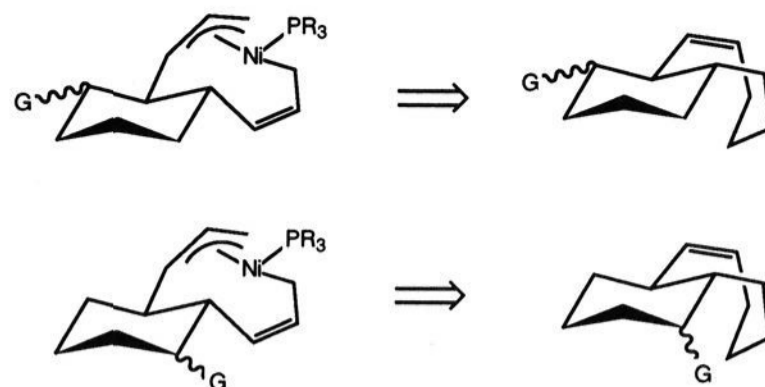
mol for the anti-allyl isomers. The syn-allyl complexes were calculated to be 2.8 kcal/mol more stable than the corresponding anti forms. It is recognized that these simple prototypical models do not account for the possibility of steric interactions between phosphine substituents and the rest of the complex that may also factor into the equilibrium composition. Nevertheless, the relative energy values are in good qualitative and quantitative agreement with published experimental data[15] for syn/anti-allyl equilibria in closely related nickel complexes (0.4–1.6 kcal/mol, favoring the syn isomer).

II. Application to Intramolecular Cyclodimerizations. On the premise that steric interactions among the various reactive conformations of these ground-state allyl nickel complexes might influence the diastereoinduction of intramolecular nickel-catalyzed cycloadditions, we determined the global minimum-energy conformations for all reasonable diastereomers. This included exploring all possible rotors of the particular substituent. The lowest energy conformers of the various cyclohexyl-fused complexes (**10–14**) were used to derive the corresponding substituted complexes.

For the preliminary evaluation of the various models for correlation with product diastereoselectivities, homoallylic-substituted systems with either CN, Me, CH_2OAc, or CO_2Me as substituents were examined. There are two possible structures available for each diastereomer differing in the position of the substituent relative to that of the π-allyl moiety as illustrated for the η^1,η^3-bis-allyl complex in Scheme 2. In the products, due to the concave nature of the chair–twist boat equilibrium conformation,[9b] this translates into a difference in the relationship of the substituent to the concavity of the cyclooctadiene portion.

To evaluate these models, the relative energies of diastereomeric intermediates were compared to observed stereochemical ratios. Only the global conformational minima were used to determine relative energies. The calculated differences in steric energy were taken to be an approximation of the free energy differences for these complexes and used to predict the expected diastereomeric ratios. In each case examined, equatorial-substituted isomers were the energetically favored. For the bis-η^3-complexes, structures with axial substituents on the convex face were the lower energy structures. The alternate arrangements were generally around 1 kcal/mol less stable.

Goodness of fit was based on linear regression coefficients obtained from the corresponding plots of observed versus calculated diastereoselectivities for the various model complexes: **10**, $r = 0.07$; **11**, $r = 0.05$; **12**, $r = 0.07$; **13a**, $r = 0.21$; **14a**, $r = 0.99$; **14b**, $r = 0.24$ (for the case where axial substituents are on the convex face). Best agreement with both the experimentally determined sense and degree of diastereoinduction was obtained using substituted models derived from **14a**. Tables 2–5 list the results of this study. There appears to be no good correlation between the steric energy differences and the observed diastereoselectivities using any of the bis-η^3-allyl models.
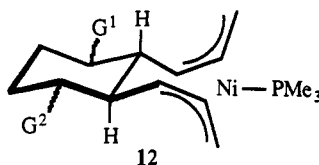
We next examined a more realistic situation including the triphenylphosphine ligand in order to gauge the influence of the phosphorus substituents on the calculated steric stabilities of these isomers. This involved determining the energetically preferred

π-Allyl Intermediates in Ni(0)-Catalyzed Cycloadditions

J. Am. Chem. Soc., Vol. 116, No. 1, 1994   335

Table 2. Relative MM2 Energies and Calculated Diastereoselectivities Using Syn-bis-η³-allyl (**10**) and Anti-bis-η³-allyl Models (**11**)
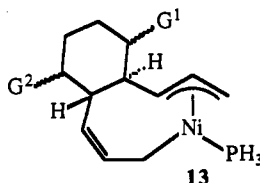

G¹	G²	model[a]	ΔE_s[b] ($G_{ax} - G_{eq}$)	calc ratio[c] (G_{eq}/G_{ax})	obsd ratio[d] (G_{eq}/G_{ax})
CN	H	10	0.3	1.6:1	1.5:1
Me	H	10	2.4	38:1	20:1
CH₂OAc	H	10	2.8	69:1	21:1
CO₂Me	H	10	2.1	24:1	>70:1
H	CN	10	0.3	1.6:1	1.5:1
H	Me	10	1.9	18:1	20:1
H	CH₂OAc	10	2.0	21:1	21:1
H	CO₂Me	10	1.4	8:1	>70:1
CN	H	11	0.6	2.5:1	1.5:1
Me	H	11	2.8	69:1	20:1
CH₂OAc	H	11	3.1	108:1	21:1
CO₂Me	H	11	2.2	28:1	>70:1
H	CN	11	0.6	2.5:1	1.5:1
H	Me	11	2.5	44:1	20:1
H	CH₂OAc	11	3.1	108:1	21:1
H	CO₂Me	11	2.3	32:1	>70:1

[a] The basic model from which the substituted cases are derived. [b] Calculated steric energy differences are given in kcal/mol. [c] Stereoinduction ratios calculated at a reaction temperature of 60 °C. [d] Reference 9c.
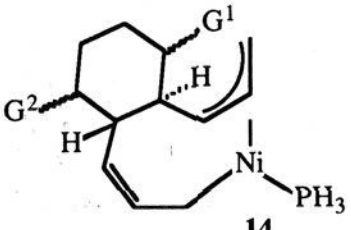
Table 3. Relative MM2 Energies and Calculated Diastereoselectivites Using Bis-anti Model 12

G¹	G²	model[a]	ΔE_s[b] ($G_{ax} - G_{eq}$)	calc ratio[c] (G_{eq}/G_{ax})	obsd ratio[d] (G_{eq}/G_{ax})
CN	H	12	0.5	2.1:1	1.5:1
Me	H	12	2.7	59:1	20:1
CH₂OAc	H	12	3.1	108:1	21:1
CO₂Me	H	12	2.1	24:1	>70:1

[a] The basic model from which the substituted cases are derived. [b] Calculated steric energy differences are given in kcal/mol. [c] Stereoinduction ratios calculated at a reaction temperature of 60 °C. [d] Reference 9c.

Table 4. Relative MM2 Energies and Calculated Diastereoselectivities Using Syn-model 13

G¹	G²	model[a]	ΔE_s[b] ($G_{ax} - G_{eq}$)	calc ratio[c] (G_{eq}/G_{ax})	obsd ratio[d] (G_{eq}/G_{ax})
CN	H	13a	1.1	5:1	1.5:1
Me	H	13a	2.9	80:1	20:1
CH₂OAc	H	13a	3.4	170:1	21:1
CO₂Me	H	13a	2.5	44:1	>70:1
H	CN	13a	1.2	6:1	1.5:1
H	Me	13a	3.8	311:1	20:1
H	CH₂OAc	13a	4.1	490:1	21:1
H	CO₂Me	13a	2.5	44:1	>70:1
CN	H	13b	0.2	1.4:1	1.5:1
Me	H	13b	1.5	10:1	20:1
H	CN	13b	0.7	3:1	1.5:1
H	Me	13b	2.9	80:1	20:1

[a] The basic model from which the substituted cases are derived. [b] Calculated steric energy differences are given in kcal/mol. [c] Stereoinduction ratios calculated at a reaction temperature of 60 °C. [d] Reference 9c.
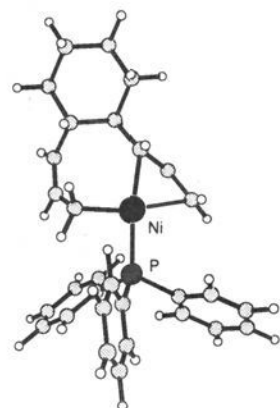
rotor conformations of the three phenyl rings for each type of complex. The method used was to drive the dihedral angles of the individual phenyl–phosphorus bonds and the nickel–phosphorus bond through 180° to ensure we located the lowest possible conformation of the ligand for the various complexes. Exami-

nation of the individual structures (at 30-deg increments) generated by this process revealed two noteworthy features: (1) a concerted movement of the three phenyl rings occurs such that driving one ring through 180° also results in the net rotation of the other two rings by 180° and (2) there is also a so-called "slip
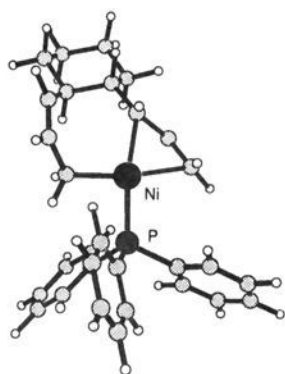
Table 5. Relative MM2 Energies and Calculated Diastereoselectivites Using Anti-model 14

14

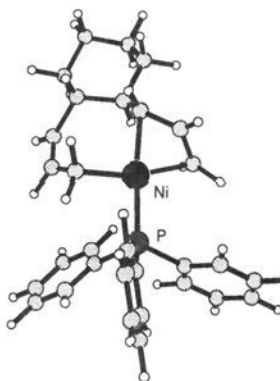| G^1	G^2	model[a]	$\Delta E_s{}^b$ ($G_{ax} - G_{eq}$)	calc ratio[c] (G_{eq}/G_{ax})	obsd ratio[d] (G_{eq}/G_{ax})
CN	H	**14a**	1.0	5:1	1.5:1
Me	H	**14a**	2.2	28:1	20:1
CH$_2$OAc	H	**14a**	2.2	28:1	21:1
CO$_2$Me	H	**14a**	2.9	80:1	>70:1
H	CN	**14a**	0.6	2:1	1.5:1
H	Me	**14a**	2.9	80:1	20:1
H	CH$_2$OAc	**14a**	3.7	268:1	21:1
H	CO$_2$Me	**14a**	1.7	13:1	>70:1
CN	H	**14b**	2.0	21:1	1.5:1
Me	H	**14b**	6.2	1.2×10^4:1	20:1
CH$_2$OAc	H	**14b**	5.8	6.4×10^3:1	21:1
CO$_2$Me	H	**14b**	4.3	662:1	>70:1
H	CN	**14b**	0.6	2:1	1.5:1
H	Me	**14b**	2.8	69:1	20:1
H	CH$_2$OAc	**14b**	3.2	126:1	21:1
H	CO$_2$Me	**14b**	1.9	18:1	>70:1

[a] The basic model from which the substituted cases are derived. [b] Calculated steric energy differences are given in kcal/mol. [c] Stereoinduction ratios calculated at a reaction temperature of 60 °C. [d] Reference 9c.
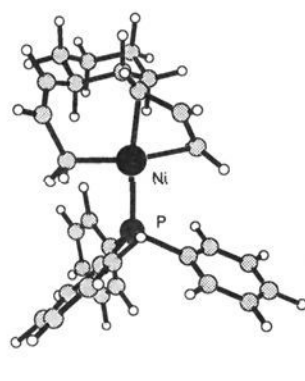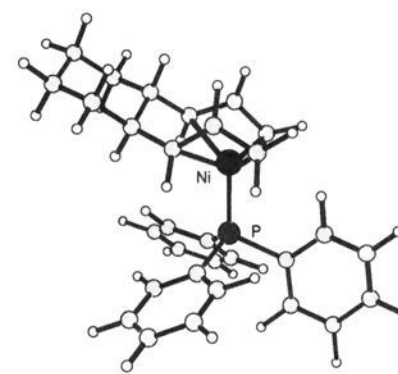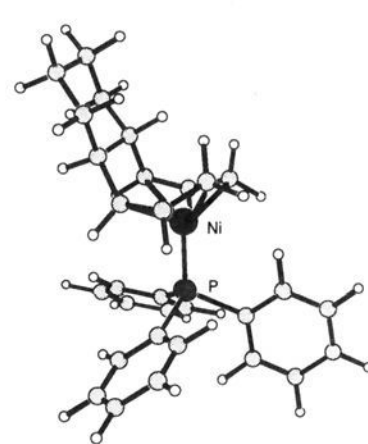

15a

15b

17

16a

16b

18

19

Figure 7. MM2-minimized structures of the lowest energy conformations for η^3,η^3-bis-allyl complexes **17**, **18**, and **19**.

Figure 6. MM2-minimized structures of the lowest energy conformations for η^1,η^3-bis-allyl complexes **15** and **16**.
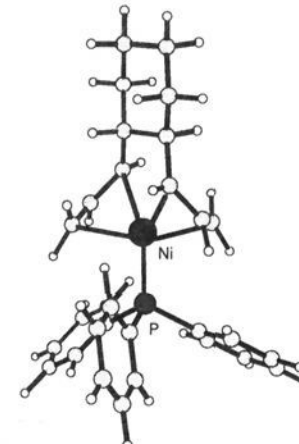
cog" movement in which 180° rotation of two rings occurred without a net rotation of the third. Generally, the MM2 calculated barrier to rotation about the phenyl–phosphorus bond was around 2–3 kcal/mol and that about the nickel–phosphorus bond approximately 3–5 kcal/mol. In all but three models, the counterclockwise rotor was slightly favored over the clockwise rotor (see Figures 6 and 7). The calculated energy differences between the right-hand and left-hand rotors were all less than 1 kcal/mol, which is consistent with experimental values. The right-hand and left-hand screw configurations in organometallic complexes typically differ by less than 1 kcal/mol, and the helicity reversal process has a low energy barrier.[26]
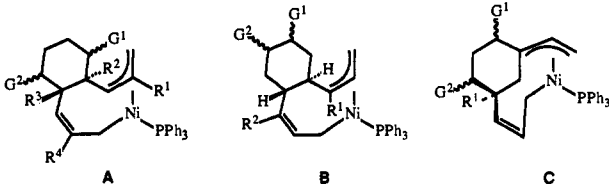
From the preliminary results (Tables 2–5), it is clear that model **14** is more viable as a predictive tool than **10–13**. Therefore, the triphenylphosphine analog **16a** was selected as our working model for further investigations. Table 6 summarizes our findings. For allylic substituents on the starting tetraene, there was an excellent correspondence between the calculated energy differences with

(26) (a) Davies, S. G.; Derome, A. E.; McNally, J. P. *J. Am. Chem. Soc.* **1991**, *113*, 2854–2861. (b) Hunter, G.; Weakley, T. J. R.; Weissensteiner, W. J. *Chem. Soc., Dalton Trans.* **1987**, 1545–1550. (c) Jones, W. D.; Feher, F. J. *Inorg. Chem.* **1984**, *23*, 2376–2388. (d) Docherty, J. B.; Rycroft, D. S.; Sharp, D. W. A.; Webb, G. A. *J. Chem. Soc., Chem. Commun.* **1979**, 336–337. (e) Faller, J. W.; Johnson, B. V. *J. Organomet. Chem.* **1975**, *95*, 99–113. (f) Stanley, K.; Zelonka, R. A.; Thomson, J.; Fiess, P.; Baird, M. C. *Can. J. Chem.* **1974**, *52*, 1781–1786. (g) Brown, J. M.; Mertis, K. *J. Organomet. Chem.* **1973**, *47*, C5–C7 and references therein.

Table 6. Relative MM2 Energies and Calculated Diastereoselectivities from Model 16a

G¹	G²	R¹	R²	R³	R⁴	complex type	$\Delta E_s{}^a$ ($G_{ax} - G_{eq}$)	calc ratio^b (G_{eq}/G_{ax})
CN	H	H	H	H	H	A	0.8	3:1
Me	H	H	H	H	H	A	1.9	18:1
CH₂OAc	H	H	H	H	H	A	2.1	24:1
CO₂Me	H	H	H	H	H	A	2.9	80:1
H	CN	H	H	H	H	A	0.3	2:1
H	Me	H	H	H	H	A	2.2	29:1
H	CH₂OAc	H	H	H	H	A	2.2	29:1
H	CO₂Me	H	H	H	H	A	1.4	8:1
CO₂Me	H	H	H	Me	H	A	3.6	230:1
H	CO₂Me	H	Me	H	H	A	3.6	230:1
CO₂Me	H	Me	H	Me	H	A	3.3	170:1
H	CO₂Me	H	Me	H	Me	A	4.8	1410:1
OTBDMS	H	H	H			B	−2.3	1:32
H	OTBDMS	H	H			B	0.0	1:1
OAc	H	H	Me			B	−0.2	1:1.4
H	OAc	Me	H			B	−0.4	1:2
OTBDMS	H	H				C	0.3^c	1.5:1^c

^{a} Differences in steric energy between the axial and equatorial substituents are given in kcal/mol. ^{b} Calculated at a reaction temperature of 60 °C. ^{c} Reaction temperature of 110 °C.

the observed diastereoselectivity from structures in which the position of the substituent is adjacent to that of the π-allyl moiety. The energy difference between the two substituent orientations in this structure was mainly due to unfavorable van der Waals interactions in the axial isomer. However, with the axial carbomethoxy substituent there is a superposition of van der Waals and torsional strain due to the inability of this substituent to adopt the preferred eclipsed conformations[27] in this steric environment, which is absent in the equatorial isomer.

In the case of homoallylic substituents, our model predicts essentially no stereoselectivity. There are only two reported examples for comparison, both with oxygen substituents.[9a] In contrast to experimental results, our force field calculations consistently favor the axial orientation for these ethers, although only slightly. The last entry of Table 6 arises from a different type of substrate where one end of the connecting tether is attached at an internal carbon. There was only one low-energy arrangement for the corresponding bis-allyl nickel complex, that in which the bridgehead carbon is part of the π-allyl system. The other option, where the bridgehead carbon is involved in a double bond, was over 5 kcal/mol higher in energy. A twist boat conformation is adopted by the six-membered ring. The lower energy diastereomer has the substituent syn to the methano bridge, and the predicted stereoselectivity agrees well both in direction and magnitude with the experimentally observed stereoinduction.[9b]

Although we have not proven the origins of stereocontrol to lie solely within this complex, our study does suggest that similar steric interactions may be involved in the stereodiscriminating step and provides a direction for further study of this complex reaction. This work also provides a simple model for predicting the stereochemical outcome. For easy comparison of the reliability of our working model, Table 7 summarizes the predictions we have made along with the available experimental results. Except for the anomalous ether-substituted cases, diastereoselectivities are extremely well reproduced both qualitatively and quantitatively by this model (linear regression coefficients were 0.97 and 0.84, excluding and including type B products, respectively).

On the basis of these results, it may be likely that the product-determining step for this process is the reaction of these complexes

(27) For a review, see: Testa, B. *Principles of Organic Stereochemistry*; Dekker: New York, 1979; pp 97–105.

and the differences in strain energy are maintained in the diastereomeric transition states. This reductive elimination would presumably be the first irreversible step, and thus the relative concentrations and respective rates of reductive elimination govern the stereochemical preferences of the product. We are currently examining this issue and others directly related to the nature of this transition structure.

III. Application to the Cyclodimerization of *trans*-Piperylene. The nickel-catalyzed dimerization of *trans*-piperylene provides an opportunity to examine factors involved in both the regio- and stereoselectivity of this transformation. Control of regioselectivity in the initial coupling mode and of the isomeric product composition to form the bis-allyl complex (Scheme 3) has both electronic and steric components.[11,12] Complexes **20** and **21** [L = PPh₃, P(C₆H₁₁)₃] have been isolated from stoichiometric reactions and are conceivably the more stable isomers. The trans orientation of the methyl groups in complex **20** has been confirmed by X-ray crystallography.[11] Intermediates such as **22**, derived from head-to-head coupling of the piperylene molecules, have not been observed. Apparently this mode does not occur due to unfavorable electronic or steric factors in the preceding bis-diene complex or the substituted η¹-moiety in **22**. Therefore, head-to-head adducts were excluded from our analysis.

The relative rates of formation of **20** and **21** are unknown, and it has not been possible to determine them indirectly from the product composition.[12] These intermediates do not represent the final step in the reaction, since the syn arrangement of the π-allyl substituents would lead to a trans double bond in the product. Isomerization to the anti arrangement must occur before the final reductive coupling. Syn/anti isomerization in organometallic complexes is known to be a rather facile process.[13,18]

We tested our η¹,η³-bis-allyl model to this system to determine if there is any correlation, based on steric grounds, between the lowest energy isomers of the various dimethyl-substituted systems and the experimentally observed substitution patterns. The lowest energy conformers of the butadiene complexes, **23** and **24**, were used to derive the corresponding dimethyl-substituted complexes (see Figure 8). Calculations were carried out for both cis and trans orientations of the methyl groups to gain insight into their relative steric energies. The results of our calculations (Table 8) indicate that trans-oriented dimethylcycloocta-1,3-diene (DM-

Table 7. Comparison between Experiment and Predicted Product Stereoselectivities[a]

G^1	G^2	R^1	R^2	product type	calc ratio (G_{eq}/G_a3x)	exp ratio (G_{eq}/G_{ax})
CO_2Me		H	H	A	80:1	>70:1
Me		H	H	A	18:1	20:1
CN		H	H	A	3:1	1.5:1
CH_2OAc		H	H	A	24:1	21:1
CO_2Me		Me	H	A	230:1	>70:1
CO_2Me		Me	Me	A	170:1	>70:1
OAc		H	H	A	9:1	*
NHAc		H	H	A	6:1	*
$COCH_3$		H	H	A	29:1	*
OTBDMS		H		B	1:1	1.7:1
OAc		Me		B	1:2	2.2:1
$OSiMe_3$		H		B	1.4:1	*
OCH_2Ph		H		B	1:1.6	*
CO_2Me		H		B	3.3:1	*
H	OTBDMS	H		C	$1.5:1^b$	$1.3:1^b$
H	$OSiMe_3$	H		C	$8:1^b$	*
OTBDMS	H	H		C	$5:1^b$	*

[a] Stereoinduction ratios were calculated at a reaction temperature of 60 °C unless otherwise stated. [b] Reaction temperature of 110 °C.

23   **24**
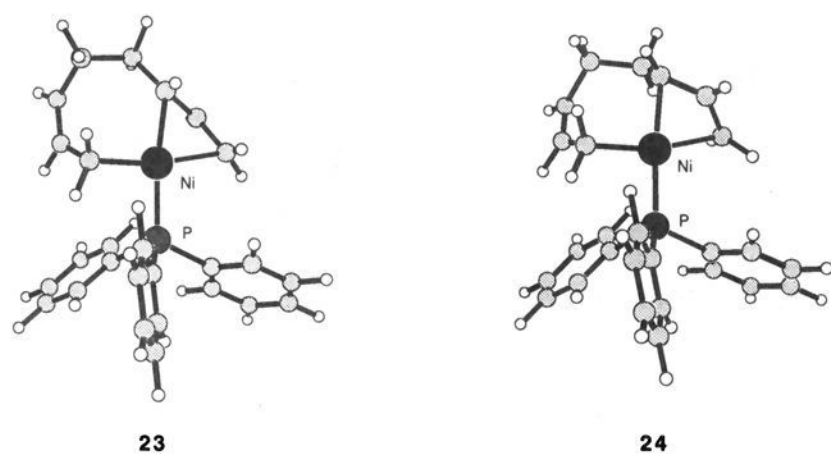
Figure 8. MM2-minimized structures of model complexes **23** and **24**.

Scheme 3. Correlation between Coupling Mode and Product Stereochemistry
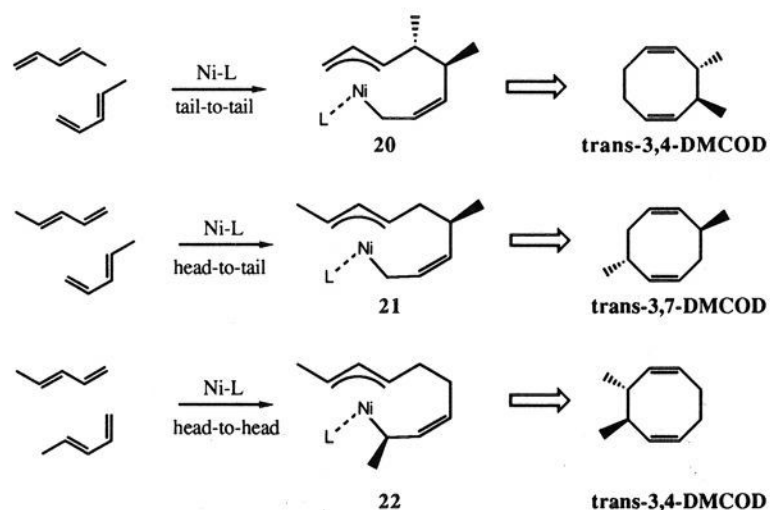
COD) products should be predominant over the cis isomers if the relative stabilities of the regioisomeric η^1,η^3-bis-allyl complexes are important.

Interestingly, this model predicts the two experimentally observed complexes[12] (**20** and **21**) to be the overall most stable steric arrangements. Whether on the basis of the syn or anti model system, these same two isomers were consistently lowest in energy. One (R^1, R^4 = Me) would be expected to ultimately give rise to *trans*-3,4-DMCOD and the other (R^4, R^5 = Me) to *trans*-3,7-DMCOD (cf. Scheme 3). The differences in steric

energies between the corresponding syn and anti models of identical substitution pattern are also listed in Table 8. In all but one case (R^3, R^5 = Me), the syn model was lower in energy than the anti model.

Experimentally, *trans*-DMCOD isomers are formed either predominantly or exclusively, depending on the reaction conditions; however, there are conflicting reports as to the regioisomeric composition.[12b,28] Work by Tolstikov indicates the major isomer formed from *trans*-piperylene dimerization (no reaction temperature given) was *trans*-3,7-DMCOD in a constant ratio of 6:1 with respect to the *trans*-3,4-DMCOD isomer.[28] Heimbach and Hey found that *trans*-3,4-DMCOD was the major isomer formed (64–75%) at 30 °C using several different phosphorus ligands.[12b] Heimbach proposes a different pathway for COD formation via nickel-catalyzed Cope rearrangement of initially formed divinylcyclobutane isomers.

Of note are the predictions of our modeling study. Assuming a reaction temperature of 30 °C, the calculated regioisomeric product composition based on the anti-allyl model would be 5.2:1 favoring the 3,7-isomer, which is in good agreement with the Tolstikov data. However, the predicted regioselectivity is reversed on the basis of the syn-allyl model becoming 3.2:1 favoring the 3,4-isomer, which is in good agreement with Heimbach's results. The source of Ni(0) was different in these two studies. Heimbach employed $Ni(COD)_2$ whereas Tolstikov used an organoaluminum reducing agent/Ni(II) catalyst system. This suggests the organoaluminum species may have some role in the selectivity.

Assuming that the relative rates of the formation or subsequent collapse of these regioisomeric complexes control the stereochemical outcome, we may expect to find a correlation if ground-state preferences are maintained in the isomeric transition structures. Therefore, the stereochemistries and regiochemistries of piperylene dimerization could be interpretable in terms of the relative stabilities of the η^1,η^3-complexes. This would be consistent with several plausible scenarios: (1) the reversible formation of the initial syn-allyl complexes is rate determining, and the coupling mode is determined by the relative thermodynamic stabilities of the syn-allyl complexes; (2) reversion of the anti-allyl forms to the syn-allyl forms is faster than reaction to form products (i.e.,

(28) Tolstikov, G. A.; Dzhemilev, U. M.; Ivanov, G. E. *Zh. Org. Khim.* **1975**, *11*, 984–989.

Table 8. Model Structures and Relative Energies of Dimethyl-η^1,η^3-octadienyl Nickel Triphenylphosphine Complexes

derived from syn model **23**   derived from anti model **24**
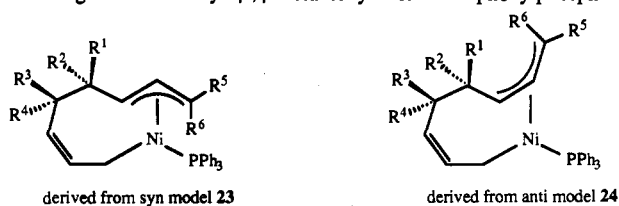
		relative energies[a]			
R^n = Me	mode	syn	anti	$\Delta E_s{}^b$ (anti – syn)	product
1,4	tail-to-tail	0.0	2.7	2.7	*trans*-3,4-DMCOD
2,3	tail-to-tail	3.5	5.6	2.1	*trans*-3,4-DMCOD
3,6	head-to-tail	3.3	6.4	3.1	*trans*-3,7-DMCOD
4,5	head-to-tail	0.5	1.8	1.3	*trans*-3,7-DMCOD
1,3	tail-to-tail	1.8	2.8	1.0	*cis*-3,4-DMCOD
2,4	tail-to-tail	1.3	4.8	3.5	*cis*-3,4-DMCOD
3,5	head-to-tail	3.3	2.8	–0.5	*cis*-3,7-DMCOD
4,6	head-to-tail	0.7	4.2	3.5	*cis*-3,7-DMCOD

[a] Energies in kcal/mol and given relative to the lowest energy regioisomer of the syn model. [b] Difference in steric energy (kcal/mol) is between the corresponding anti and syn models of the same regioisomer.

the reductive elimination is rate determining), and regioselectivity is driven by the relative thermodynamic stabilities of the anti-allyl complexes. A possible explanation for the difference in the observed regiochemistry with the aluminum and aluminum-free nickel catalysts could thus be due to a change in the mechanism such that (1) applies under Heimbach's conditions and (2) applies for the Tolstikov case. These ideas await experimental verification.

Conclusion

While there is still no definitive answer to the origin of stereoselectivity in this reaction, our results indicate the product stereochemistry in nickel-catalyzed [4 + 4] cycloadditions can be predicted by the relative stabilities of diastereomerically related η^1,η^3-bis-allyl nickel intermediates. This provides a quantitative predictive tool for planning other applications of this reaction. It should also be noted that our study has primarily focused on reaction conditions that involve the triphenylphosphine ligand present in a 2:1 ratio with respect to the nickel concentration. It is well-known that the reaction is sensitive to the phosphine and its concentration. Changing the nature of the phosphine may change the nature of the stereochemically discriminating species

and thus the observed diastereoselectivities. Investigation of this issue, including bis-allyl nickel diphosphine intermediates and reductive elimination transition structures, and further detailed modeling studies of this reaction class with other metals are in progress.

Force field modeling of organometallic reactions is severely hampered by the current lack of legitimate parameters for these type of systems and the prevailing attitude that transition metal species are not generally amenable to force field methods. We hope that this paper will provide an enlightened view of the potential this method holds for understanding structure and steric energies of organometallic species and act as a catalyst for further theoretical and experimental investigations which are crucial for progress in this area.